ARTICLE

Performance enhancement through post-treatments of CdS-sensitized solar cells fabricated by spray pyrolysis deposition

Yong Hui Lee,[†,‡] Sang Hyuk Im,[†] Jae Hui Rhee,[†] Jong-Heun Lee,[‡] and Sang Il Seok*[,†]

[a] KRICT-EPFL Global Research Laboratory, Advanced Materials Division, Korea Research Institute of Chemical Technology, 19 Sinseongno, Yuseong, Daejeon 305-600, Republic of Korea, and Department of Materials Science and Engineering, Korea University, Anam-Dong, Sungbuk-Gu, Seoul 136-713, Republic of Korea

ABSTRACT The CdS-sensitized solar cells (CdS-SSC) were fabricated by spray pyrolysis deposition (SPD) method. The performance of the cells was greatly improved through post-treatments that included thermal oxidation at 500 °C for 30 min in an air atmosphere and subsequent chemical etching by 40 mM aqueous HCl solution at room temperature for 30 min, as compared to as-deposited CdS-SSC. The CdS-SSC in a I^-/I_3^- electrolyte system was resulted in the improvement of J_{sc} (3.3 → 5.2 mA/cm^2), V_{oc} (697 → 758 mV), FF (41.4% → 46.9%), and (0.95% → 1.84%). Similarly, the efficiency of CdS-SSC in a noncorrosive polysulfide electrolyte system was also enhanced by the proposed thermal oxidation and etching process. The increase in the cell efficiency is attributed to the reduced charge recombination among sensitizer themselves through the mitigation of overaggregated CdS sensitizers deposited by SPD.

KEYWORDS: quantum dot-sensitized solar cell • cadmium sulfide • cadmium oxide • spray pyrolysis deposition • oxidation, etching.

1. INTRODUCTION

Recently, quantum dot-sensitized solar cells (QDSSCs) have been considered as a possible alternative to dye-sensitized solar cells (DSSCs) (1) because semiconductor quantum dots (QDs) exhibit outstanding properties such as a high extinction coefficient, efficient charge separation, spectral tunability by particle size, good stability, and multiple exciton generation (2). In particular, the metal chalcogenide QDs such as PbS, CdS, CdSe, CdTe, and CIS have been extensively studied and there has been a significant improvement in the efficiency of solar cells having these QDs (3−10). So far, the QDs have been successfully incubated onto a mesoporous TiO_2 (mp-TiO_2) surface by chemical bath deposition (CBD), successive ionic layer adsorption and reaction (SILAR) and photodeposition method (3, 4, 11). Recently, a photodeposition technique has been shown to be promising for preparing metal calcogenide-TiO_2 heterojunction systems. Despite many advantages of a spray pyrolysis deposition (SPD) method such as a contamination-free chemical bath and a simple and readily commercializable process, SPD methods have not attracted attention probably because of the difficulties of controlling the aggregation of sensitizing particles deposited onto the mp-TiO_2 surface. Because the generated charge carriers in the aggregated sensitizing particles could not be effectively transported, their consequent recombination was inevitable because of the abundant surface traps and insufficient pathway for charge carriers. Hence, it is important to devise a way to fabricate an efficient QDSSC by the SPD method. There are two suggested methods for solving the problem of the aggregation of sensitizing particles in the SPD method. One is to *in situ* coat the sensitizing particles on the mp-TiO_2 surface as a thin layer by using the state-of-art level control of the SPD method. The other is to isolate overaggregated sensitizers on the mp-TiO_2 surface by chemical-etching. Here, we report on the enhancement of the performance of CdS-sensitized solar cells fabricated by spray pyrolysis deposition through post-treatments such as oxidation and chemical etching.

2. EXPERIMENTAL SECTION

Preparation of TiO_2 paste. For the mp-TiO_2 electrode, TiO_2 nanoparticles were synthesized by using a precipitation method. $TiCl_4$ (Titanium(IV) chloride, 99.9%, Aldrich) was diluted to form a 3 M aqueous solution with double-distilled water (D-water) in an ice bath and was further diluted to form a 0.5 M aqueous solution before the precipitation. For the precipitation, the 0.5 M aqueous solution of $TiCl_4$ and NH_4OH (Ammonium hydroxide solution, Samchun Pure Chemicals, 28.0%∼30.0%) was dropped into 100 mL of deionized (DI) water at the same time while maintaining the pH at 3−4. Then, the pH of the reactant was increased to 9.0 by adding additional NH_4OH while stirring vigorously. The solution was then heated at 90 °C for 3 h with stirring and filtered. To remove the Cl^- ions thoroughly, the precipitate was rinsed more than three times with fresh DI water and dried for 12 h in a convection oven. To change the amorphous phase into a crystalline phase, the dried TiO_2 powder was sintered at 500 °C for 3 h in a furnace. The particle size and the specific surface area measured using a transmission electron microscope (TEM) and a BET analysis were 30−40 nm

* To whom correspondence should be addressed. E-mail: seoksi@krict.re.kr.
Received for review March 01, 2010 and accepted May 19, 2010
† Korea Research Institute of Chemical Technology.
‡ Korea University.
§ These authors have contributed equally to this work.
DOI: 10.1021/am100169t

Published on Web 06/02/2010

Scheme 1. Schematic representation of the proposed oxidation and etching method

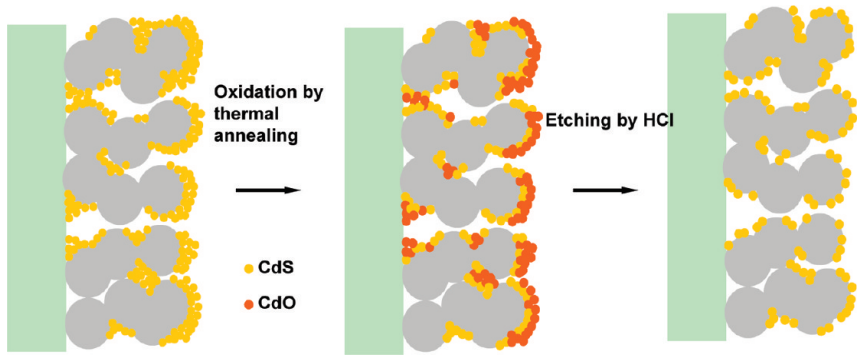

and 44−45 m^2/g, respectively. TiO_2 paste was prepared as described elsewhere (12).

Deposition and post-treatments of CdS layer. The mp-TiO_2 electrodes were screen-printed on a cleaned FTO (Pilkington, TEC15) substrate and sintered at 500 °C for 30 min. The thickness of the screen-printed electrode measured using a scanning electron microscope (SEM) was c.a. Eight μm.

For the SPD of the CdS layer, an aqueous solution of 0.1 M $CdCl_2$ and 0.13 M thiourea was sprayed on a preheated mp-TiO_2 substrate of 450 °C in an air atmosphere. 0.17 mL of the precursor solution was sprayed and was left for 10 s to form crystalline CdS particles within the mp-TiO_2 layer in 1 cycle. To increase the amount of the deposited sensitizer, we carried out 5 cycles of SPD. To isolate the overaggregated CdS layer into a thin CdS layer, the as-deposited CdS on mp-TiO_2 was thermally annealed at 500 °C for 30 min in an air atmosphere for oxidation, cooled down to room temperature, and then etched by using a 40 mM aqueous HCl solution at room temperature for 30 min.

Fabrication of CdS-SSC. The Pt-coated counter electrode was prepared by dropping 5 mM H_2PtCl_6 in *i*-propanol onto FTO glass and heating it at temperatures up to 400 °C for 10 min. The cells were assembled by sandwiching the CdS layer deposited on the mp-TiO_2 substrate and the Pt-coated counter electrode using a thermal adhesive film (Surlyn, 60 μm, DuPont). For the I^-/I_3^- electrolyte, a solution containing 0.60 M 1-butyl-3-methylimidazolium iodide (BMII, Merck), 0.03 M I_2 (Sigma-Aldrich), 0.1 M guanidine thiocyanate (Sigma-Aldrich), and 0.5 M 4-*tert*-bythylpyridine (Aldrich) in the mixture of acetonitrile and valeronitrile with a volume ratio of 85:15 was used as the redox electrolyte. In the case of the polysulfide electrolyte, a methanol/water (7:3 v/v) solution containing 0.5 M Na_2S, 2 M S, and 0.2 M KCl was used as the redox electrolyte (13). The electrolyte was injected by vacuum backfilling, prior to sealing the hole with a Surlyn film and a cover glass. In order to improve electrical contact, lead contact pads were made on both sides of electrodes by using an ultrasonic soldering iron. The active area of the photoelectrode was found to be 0.18 cm^2.

Device characterization. The photocurrent−voltage (*I-V*) characteristics of the cells were measured under illumination of 1 sun (AM 1.5G, 100 mW/cm^2) with a solar simulator (Newport, Class A, 91195A) using a Keithley 2420 sourcemeter and a calibrated Si-reference cell (certified by NREL). The external quantum efficiency (EQE) was also measured by a fully computerized home-designed system comprising a light source (300W Xe lamp, Newport, 66902) with a monochromator (Newport cornerstone 260) and a multimeter (Keithley 2001). All measurements were carried out at least five times and averaged.

3. RESULTS AND DISCUSSION

To solve the problem of the severe aggregation of CdS QDs on the mp-TiO_2 surface during the SPD method, we propose a novel method, illustrated in Scheme 1. The proposed method is composed of two steps—oxidation and etching. The first oxidation step involves the oxidation of the aggregated CdS QDs from their surface by thermally annealing them in an air atmosphere, and the second involves the etching away of the oxidized layer by an acidic etchant, as shown in Scheme 1. We intend to thermally anneal the aggregated CdS QDs to oxidize them because an improvement in the intimate contact at both the CdS-CdS and the CdS-TiO_2 interfaces is expected.

Figure 1 shows the scanning electron microscopic (SEM) images of (a) the mp-TiO_2 electrode surface and (b) the mp-TiO_2/CdS surface after SPD with an aqueous CdS precursor. For a successful deposition of CdS QDs onto mp-TiO_2, we have synthesized the tightly bonded TiO_2 nanoparticles by a sol−gel and precipitation method because the conventional mp-TiO_2 layer composed of P25 (Degussa) could be easily broken during the SPD process because of the relatively loose bonding between the TiO_2 nanoparticles. To improve the bonding strength between the TiO_2 nanoparticles, we sintered the precipitated amorphous TiO_2 at 500 °C for 3 h in a furnace and then finally obtained the anatase phase TiO_2 nanoparticles having a primary particle size of 30−40 nm and BET of 44−45 cm^2/g. Figure 1(a) clearly shows that the mp-TiO_2 electrode is sufficiently porous for the sprayed chemicals to quickly infiltrate within the mp-TiO_2 layer during the SPD process. The SEM surface image in Figure 1(b) apparently looks similar to that in Figure 1(a), which implies that the sprayed chemicals are well infiltrated and deposited onto the mp-TiO_2 surface without breaking the mp-TiO_2 structure. The magnified images of the insets in Figure 1 also confirm that the morphology and the porosity are maintained after the SPD of CdS. The left inset in Figure 1(b) is the front and back side photographs of the CdS-sprayed mp-TiO_2 layer. This clearly confirms a good infiltration of the CdS precursor into the mp-TiO_2 layer and the formation of CdS during the SPD process.

To check the composition and crystalline phase of the produced materials by following each step in Scheme 1, the X-ray diffraction (XRD) patterns were measured as shown in Figure 2. The XRD patterns of a pristine mp-TiO_2, CdS on a glass, and CdS on the mp-TiO_2 layer formed during SPD at 450 °C show that the pristine mp-TiO_2 particles are in the anatase phase and the CdS layer has a single hexagonal

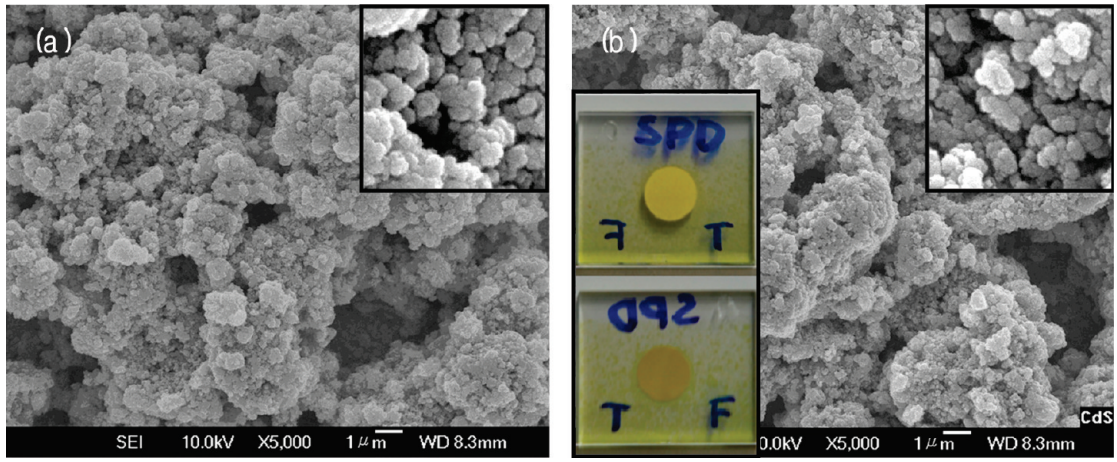

FIGURE 1. SEM surface images of (a) mp-TiO_2 and (b) as-deposited CdS on mp-TiO_2. The insets are magnified images and the photographs in the left inset in (b) shows the front and back sides of as-deposited CdS on mp-TiO_2, indicating a good infiltration of CdS within the mp-TiO_2 layer during SPD.

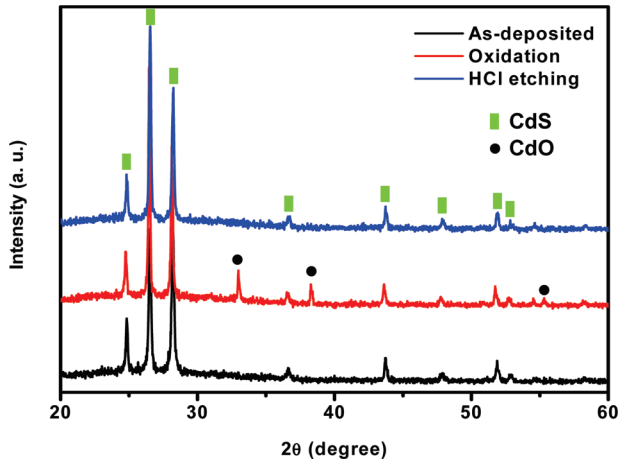

FIGURE 2. The X-ray diffraction patterns of as-deposited, oxidized and oxidized/HCl treated CdS deposited on mp-TiO_2 film.

phase of wurtzite (see Figure S1) (14). We could observe exactly the same peaks of TiO_2 and CdS after the SPD of CdS on the mp-TiO_2 electrode. This implies that the CdS is sufficiently stable to be formed by the SPD method at 450 °C in an air atmosphere. To exclude the overlapped strong TiO_2 peaks on the basis of the above experiment, we deposited the same amount of CdS on a glass substrate by using SPD method. By using this CdS film, we sequentially checked the composition of the CdS film according to the following steps of the oxidation by thermal annealing and the HCl etching, shown in Figure 2. Figure 2 clearly indicates that the pure CdS could be oxidized to CdO by thermal annealing at 500 °C for 30 min in an air atmosphere and that the CdO layer could be successfully removed by etching with 40 mM HCl at room temperature for 30 min. This oxidation and etching process could be also characterized by checking the distinctive color change with naked eyes because initially the pure CdS film reveals a light yellowish color that gradually changes to orange on the surface, which indicates the formation of the CdO layer by the oxidation of CdS on the surface, and finally recovers quickly to the light yellowish color because of the etching of the CdO layer.

To check and confirm the isolation or mitigation of the overaggregated CdS on the mp-TiO_2 surface into a thin CdS layer, we observed the transmission electron microscopic (TEM) images of CdS films, as shown in Figure 3. Figure 3 clearly shows that the overcoated CdS layer on the mp-TiO_2 layer by the SPD method could be turned into a thin or isolated CdS layers by the oxidation and etching process through the proposed scheme (see scheme 1) .

To examine the improvement in the efficiency of CdS-SSC by the proposed oxidation and etching process, we measured the current density−voltage (*J-V*) curves in the I^-/I_3^- electrolyte system, as shown in Figure 4. The power conversion efficiency (η) of the thermally annealed CdS-SSC at 500 °C for 30 min in an air atmosphere was decreased by the deterioration of the short-circuit current (J_{sc}) and the fill factor (FF) although the open-circuit voltage (V_{oc}) was increased as compared to that in the case of the as-deposited CdS-SSC ($J_{sc} = 3.3$ mA/cm^2, $V_{oc} = 697$ mV, FF = 41.4%, and $\eta = 0.95\%$), as shown in Figure 4(a), because the improved intimate contacts at the interface of TiO_2−CdS and CdS-CdS by thermal annealing might enhance the electron transport at the CdS-CdS and TiO_2−CdS interfaces by the reduction of surface trap sites. However, the severely thick oxidation layer formed by thermal annealing could hinder the extraction of holes toward the electrolyte at the same time and consequently recombine the generated charge carriers, thereby lowering J_{sc} and FF. As expected, by removing the thick oxidation layer by etching with 40 mM aqueous HCl solution for 30 min at room temperature, we could drastically increase the power conversion efficiency to 194% as compared to that in the case of as-deposited CdS-SSC through the improvement of J_{sc} (3.3 → 5.2 mA/cm^2), V_{oc} (697 → 758 mV), FF (41.4% → 46.9%), and η (0.95% → 1.84%) because the CdS layers thinned or isolated by the oxidation and etching process could effectively transport electrons and holes. The EQE in Figure 4(b) is also consistent with the results of Figure 4(a), confirming the tendency of J_{sc}.

To separate the role of oxidation by thermal annealing from that of the HCl etching because each treatment could basically remove the overdeposited CdS on the mp-TiO_2

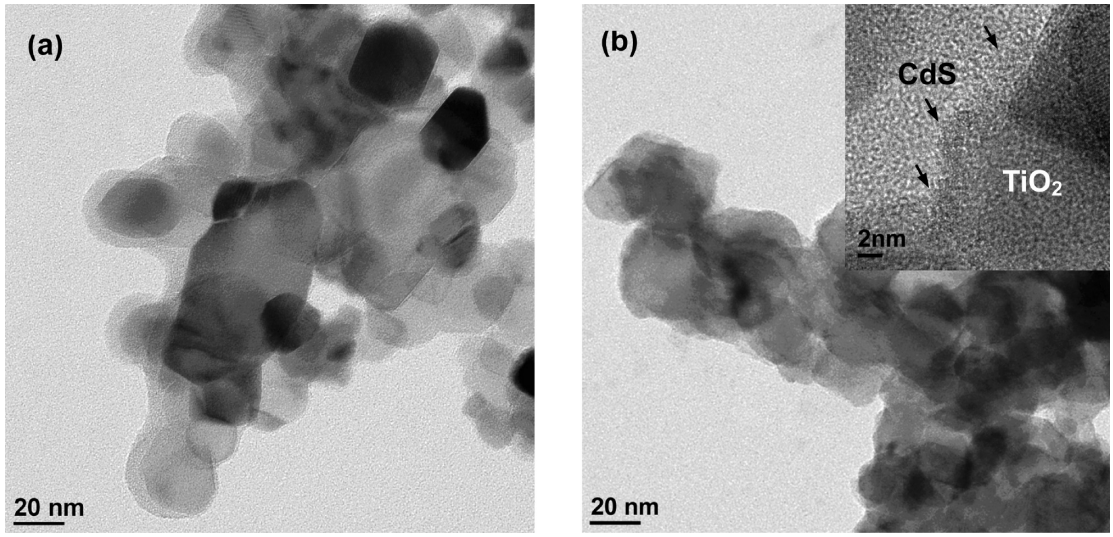

FIGURE 3. TEM images of (a) as-deposited CdS on mp-TiO_2 and (b) reconstructed CdS on mp-TiO_2 by thermal annealing and etching.

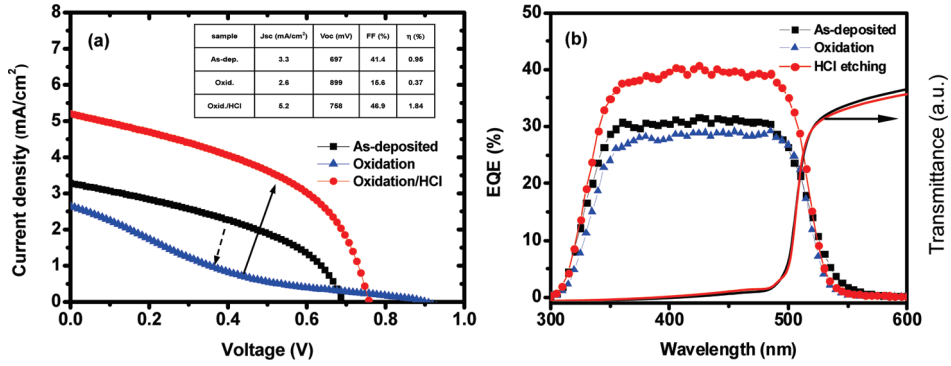

FIGURE 4. Device characterization of CdS-SSC in I^-/I_3^- electrolyte system. (a) *J-V* curves and (b) EQE and UV−visible transmittance of as-deposited (black solid line) and thermally oxidized (red solid line) CdS/mp-TiO_2 film.

layer by itself, we compared the *J-V* curve, as shown in Figure S2. The HCl etching also improved the power conversion efficiency (0.95% → 1.1%) by the enhancement of J_{sc} (3.3 → 4.4 mA/cm^2) due to the reduced charge recombination among sensitizer themselves. However, the other photovoltaic parameters deteriorated because of the relatively loose interface contacts of CdS-TiO_2 and CdS-CdS or a relatively severe recombination at the CdS-electrolyte interface or the corrosion of CdS by the I^-/I_3^- electrolyte.

To exclude the possibility of corrosion of CdS by the I^-/I_3^- electrolyte, we performed additional experiments with a polysulfide electrolyte, as shown in Figure 5. The effect of oxidation by thermal annealing and etching with HCl in a polysulfide electrolyte system was also consistent with that in the case of the I^-/I_3^- electrolyte system. The V_{oc} was increased by the thermal annealing due to improved intimate interfacial contacts and the J_{sc} (3.1 → 3.8 mA/cm^2), V_{oc} (566 → 606 mV), FF (33.8% → 37.6%), and (0.59% → 0.87%) values could be greatly improved by the HCl etching of the thermally annealed device.

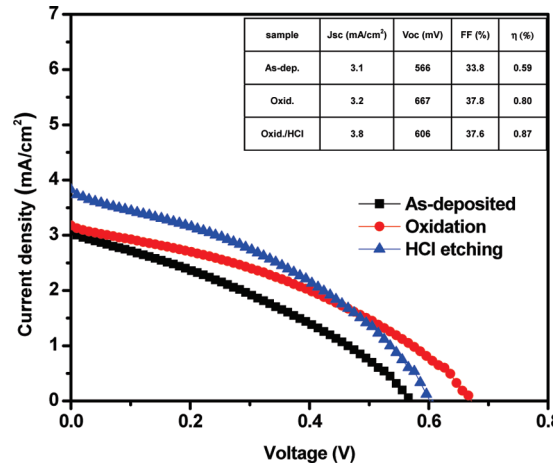

FIGURE 5. *J-V* curves of CdS-SSC in polysulfide electrolyte system.

4. CONCLUSION

The overaggregated CdS sensitizers deposited by SPD method on the mp-TiO_2 surface were successfully turned into a thin or isolated CdS layer through post-treatments, i.e., thermal oxidation at 500 °C for 30 min in an air atmosphere, followed by etching with a 40 mM aqueous HCl solution at room temperature for 30 min. The efficiency of the post-treated CdS-SSC in both I^-/I_3^- electrolyte and a noncorrosive polysulfide electrolyte system was greatly improved, because CdS layers thinned or isolated by the oxidation and etching process could effectively transport electrons and holes. This result suggests that the proposed method will provide a general solution for the fabrication of efficient QDs-SSCs through the SPD method.

Acknowledgment. This study was supported by the Global Research Laboratory (GRL) Program through the National Research Foundation of Korea funded by the Ministry of Education, Science and Technology, and by a grant from the Fundamental R&D Program for Core Technology of Materials funded by the Ministry of Knowledge Economy, Republic of Korea. The work of J. H. Lee was supported by NRL (the National Research Foundation of Korea) Program (R0A-2008-000-20032-0).

Supporting Information Available: The X-ray diffraction patterns of mp-TiO_2, CdS deposited on glass and CdS deposited on mp-TiO2, J-V curve of post-treated cell and EQE and UV−visible spectra. This material is available free of charge via the Internet at http://pubs.acs.org.

REFERENCES AND NOTES

(1) O'Regan, B.; Grätzel, M. *Nature* **1991**, *353*, 737–740.
(2) Nozik, A. J. *Chem. Phys. Lett.* **2008**, *457*, 3–11.
(3) Yafit, I.; Olivia, N.; Miles, P.; Gary, H. *J. Phys. Chem. C* **2009**, *113*, 4254–4256.
(4) Lee, H. J.; Chen, P.; Moon, S.-J.; Sauvage, F.; Sivula, K.; Bessho, T.; Gamelin, D. R.; Comte, P.; Zakeeruddin, S. M.; Seok, S. I.; Grätzel, M.; Nazeeruddin, M. K. *Langmuir* **2009**, *25*, 7602–7608.
(5) Robel, I.; Subramanian, V.; Kuno, M.; Kamat, P. V. *J. Am. Chem. Soc.* **2006**, *128*, 2385–2393.
(6) Niitsoo, O.; Sarkar, S. K.; Pejoux, C.; Ruhle, S.; Cahen, D.; Hodes, G. *J. Photochem. Photobiol. A* **2006**, *181*, 306–313.
(7) Lee, Y.-L.; Huang, B.-M.; Chien, H.-T. *Chem. Mater.* **2008**, *20*, 6903–6905.
(8) Fan, S.-Q.; Kim, D.; Kim, J.-J.; Jung, D. W.; Kang, S. O.; Ko, J. *Electrochem. Commun.* **2009**, *11*, 1337–1339.
(9) Lan, G.-Y.; Yang, Z.; Lin, Y.-W.; Lin, Z.-H.; Liao, H.-Y.; Chang, H.-T. *J. Mater. Chem.* **2009**, *19*, 2349–2355.
(10) Nanu, M.; Schoonman, J.; Goossens, A. *Nano Lett.* **2005**, *5*, 1716–1719.
(11) Fujii, M.; Nagasuna, K.; Fujishima, M.; Akita, T.; Tada, H. *J. Phys. Chem. C* **2009**, *113*, 16711–16716.
(12) Ito, S.; Murakami, T. N.; Comte, P.; Liska, P.; Grätzel, C.; Nazeeruddin, M. K.; Grätzel, M. *Thin Solid Films* **2008**, *516*, 4613–4619.
(13) Lee, Y.-L.; Chang, C.-H. *J. Power Sources* **2008**, *185*, 584–588.
(14) Cao, H.; Wang, G.; Zhang, S.; Zhang, X.; Rabinovich, D. *Inorg. Chem.* **2006**, *45*, 5103–5108.

AM100169T